Research Article | Vol. 28, No. 15 / 20 July 2020 / Optics Express 21382
Optics EXPRESS

CW demonstration of SHG spectral narrowing in a PPLN waveguide generating 2.5 W at 780 nm

LEWIS G. CARPENTER,[1,*] SAM A. BERRY,[1] ALAN C. GRAY,[1] JAMES C. GATES,[1] PETER G. R. SMITH,[1,2] AND CORIN B. E. GAWITH[1,2]

[1] *Optoelectronics Research Centre, Zepler Institute, University of Southampton, University Road, Southampton SO17 1BJ, UK*
[2] *Covesion Ltd., Premier Way, Romsey SO51 9DG, UK*
[*] *lc906@orc.soton.ac.uk*

Abstract: Periodically poled lithium niobate (PPLN) waveguides are a proven and popular means for efficient wavelength conversion. However, conventional PPLN waveguides typically have small mode field diameters (MFD) ($\lesssim$6 µm) or significant insertion and/or propagation losses, limiting their ability to operate at multi-watt power levels. In this work we utilise zinc indiffused PPLN ridge waveguides that have a larger MFD, favourable pump/SHG modal overlap, and low insertion losses. Here for the first time, we have demonstrated continuous wave (CW) spectral narrowing from a PPLN waveguide, both with high efficiency and multi-watt second harmonic generation (SHG). 2.5 W of 780 nm has been produced by SHG of an amplified 1560 nm telecom laser with a device efficiency of 58% in a 4.0-cm long ridge waveguide. We have modelled conversion efficiency and applied experimentally measured waveguide parameters to show excellent agreement to the SHG spectra. Spectral narrowing of the full width half maximum (FWHM) of 35.7% has been measured as the nonlinear drive is increased. This work demonstrates that single-pass, multi-watt, CW SHG at 780 nm is feasible from our PPLN waveguide in the large conversion regime.

1. Introduction

Armstrong, Bloembergen *et al.* gave a comprehensive explanation of nonlinear optics in their seminal paper of 1962 [1] introducing the concept of quasi-phase matching and giving a complete classical mathematical framework to describe second-order nonlinear mixing. However, for many practical uses the mathematics simplifies to a simple Fourier explanation such as the well-known second harmonic generation (SHG) tuning curves that follow the sinc^2 function. Simply, this can be understood to occur because the efficiency is low, particularly for continuous wave (CW) laser excitation. With pulsed lasers the nonlinear drive can be much greater, which in the case of SHG leads to the more complex phase matching solution representing a 'large conversion regime' or 'high nonlinear drive regime', as presented by Eimerl [2] targeted for applications of high power lasers at Lawrence Livermore National Laboratory. This high nonlinear drive regime regularly occurs in SHG of nanosecond pulsed lasers and one of its most striking effects is the spectral narrowing of the phase matching curve for SHG as comprehensively discussed by Eckardt *et al.* [3].

In periodically poled lithium niobate (PPLN) waveguides the spectral narrowing effect has been demonstrated by Parameswaran *et al.* [4] who reported a world-record 99% pump depletion in a quasi-CW regime where 50 ns pulses from a CW narrow line laser were amplified at 1 kHz repetition rate. PPLN waveguides represent one of the best systems for exhibiting SHG narrowing

#395566 https://doi.org/10.1364/OE.395566
Journal © 2020 Received 17 Apr 2020; revised 30 May 2020; accepted 1 Jun 2020; published 7 Jul 2020

Optics EXPRESS

because they have high nonlinearity, excellent power handling, and low losses [5]. At watt level operation for SHG of 1560 nm to 780 nm, PPLN waveguides have reached device efficiencies of 56% for 1.0 W at 780 nm [5,6] and a maximum reported SHG output power of 1.7 W at 34% device efficiency [7]. However, PPLN waveguides combining both multi-watt output powers and device efficiencies of >50% have not been previously reported. Watt level output powers from PPLN waveguides can be difficult to reach because of parasitic nonlinear effects such as photorefractive damage [8]. The above examples of PPLN waveguides are doped with either Mg or Zn, which is known to reduce the photorefractive effect that is more severe at shorter wavelengths [5,7,9,10]. 780 nm is the wavelength of interest within the manuscript as it is the key cooling line for Rb magneto-optical trapping [6]. Recent work in quantum technologies using Rb traps for gravitometers and magnetometers has driven development of 780 nm sources that are watt level, compact, and narrow linewidth [6].

In this paper, we discuss the design and operation of PPLN waveguides capable of generating 2.5 W of 780 nm SHG from a commercially available telecom laser at a device efficiency of 58% with a resulting demonstration of true-CW SHG spectral narrowing in a high nonlinear drive regime. Operating in full CW provides means much higher average powers than Parameswaran's work, in which the pulsed selected excitation is at least four orders of magnitude lower in terms of average power [4]. With incident powers of more than 4 W our generated SHG spectra follow the Jacobian elliptical function and are not sinc^2 in shape, which we discuss in the next section.

2. SHG in waveguides with pump depletion and propagation loss

For SHG the well-known sinc^2 output spectra is strictly only valid for an undepleted pump or a device operating within the small-conversion regime [3,4]. Numerous works detail the solution for a depleted pump or a device working within the large-conversion regime [2–4]. When working within the large-conversion regime, and with no losses, the SHG spectrum and conversion efficiency from a waveguide take the form of a Jacobian elliptic function [1,3,4]:

$$\eta = {}^{P_s(l)}\!/_{P_p(0)} = v_b^2 sn^2\left(\frac{\Gamma l}{v_b}|v_b^4\right) \tag{1}$$

$${}^{1}\!/_{v_b} = {}^{\Delta\beta}\!/_{4\Gamma} \pm \sqrt{1 + \left({}^{\Delta\beta}\!/_{4\Gamma}\right)^2} \tag{2}$$

where sn is the Jacobian elliptic function, η is the conversion efficiency, P_s and P_p are the SHG output and pump powers, l is length and Γ is the nonlinear drive (m^{-1}), the sign of the square root is chosen such that $v_b^2 \leq 1$ [3]. $\Delta\beta = \beta_s - 2\beta_p - 2\pi/\Lambda$ (m^{-1}) is the phase mismatch where β_s and β_p represents the modal propagation constants, and Λ is the grating period. Equation (1) describes the efficiency of the nonlinear interaction and by varying $\Delta\beta$ in Eq. (2), phase matching spectra can be produced in both the large and small conversion regimes. Note Eq. (1) does not account for waveguide propagation losses. The nonlinear drive is related to pump intensity by $\Gamma = \sqrt{\eta_o P_p(0)}$, where η_o is the normalised conversion efficiency ($\text{W}^{-1}\text{cm}^{-2}$). $P_p(0) = \xi P_{in}$, where ξ is the coupling efficiency and P_{in} is the incident pump power on the waveguide facet. Thus, as pump power is increased so is the nonlinear drive and this manifests itself within the SHG spectrum as spectral narrowing of the acceptance bandwidth.

When waveguide loss is present the numerical integration of coupled mode equations must be used to describe nonlinear conversion within waveguides and we follow the procedure presented by Eckardt, Byer, and Parameswaran [3,11,12]. We start by defining the electric fields in a waveguide to be $E_p(x, y, z) = A_p(z)E_p(x, y)\exp(-j\Delta\beta_p z)$ and $E_s(x, y, z) = A_s(z)E_s(x, y)\exp(-j\Delta\beta_s z)$, representing the pump and SHG. These field equations describe a positionally varying envelope function with the transverse mode eigenfields $E(x, y)$ of the waveguide, which in this case represent the fundamental pump and SHG modes. The nonlinear generation of the second harmonic and the

Optics EXPRESS

depletion of the pump can be described by the following coupled mode equations:

$$\frac{dA_s}{dz} = -j\sqrt{\eta_o}A_p^2\exp(-j\Delta\beta z) - \frac{\alpha_s}{2}A_s \tag{3}$$

$$\frac{dA_p}{dz} = -j\sqrt{\eta_o}A_p^*A_s\exp(j\Delta\beta z) - \frac{\alpha_p}{2}A_p \tag{4}$$

where A_s and A_p are the field amplitudes and $P = |A|^2$, α_s and α_p (m^{-1}) are the intensity propagation loss coefficients, and $\eta_o = \kappa^2 Iov^2$ where κ and Iov are given by:

$$\kappa = \sqrt{\frac{8\pi^2 d_{eff}^2}{n_p^2 n_s c\varepsilon_o \lambda_p^2}} \tag{5}$$

$$Iov = \frac{\iint_{-\infty}^{\infty} E_s^* E_p^2 dxdy}{\sqrt{\iint_{-\infty}^{\infty} E_s^2 dxdy}\iint_{-\infty}^{\infty} E_p^2 dxdy} \tag{6}$$

where d_{eff} is the effective nonlinearity coefficient (pm/V), n_s and n_p are the effective refractive indices of the fundamental waveguide modes of the SHG and pump, respectively. λ_p is the pump wavelength, and Iov is the overlap integral for the position-independent transverse SHG $E_s(x, y)$ and pump $E_p(x, y)$ modes profiles [13]. Equations (3) and (4) are used to provide a theoretical fit to the SHG efficiency and spectral data presented in Figs. 3 and 4.

3. Fabrication

Our approach to manufacturing PPLN waveguides is reported in our earlier works [14,15] and is based on three successive stages: zinc indiffusion to create a planar guiding layer, ultra-precision machining to form single-mode ridge waveguides, and preparation of the optical facets by dicing. The devices described in this paper were prepared in 1 mm-thick 5% magnesium-doped periodically-poled lithium niobate (MgO:PPLN) wafers (Covesion Ltd) each containing multiple 1.2 mm-wide 18.5 µm period gratings designed to access Type-0 1560-780 nm SHG via the d_{33} nonlinear coefficient. Metallic zinc was sputtered with a thickness of 100 nm on to the + z surface of each MgO:PPLN wafer (Oxford Instruments Plasma Technology, Plasma Lab System 400) and indiffused at 950 °C in an oxygen atmosphere to promote ZnO formation. To overcome any machining inaccuracy and facilitate high pump and SHG modal overlap at our chosen wavelengths, five ridge widths were cut into each PPLN grating ranging from 11-13 µm in 0.5 µm steps and parallel to the [100] X direction of the crystal [14,15]. Individual chips measuring 4.0 cm-long by 5 mm-wide were singulated from the wafer [Fig. 1(a)] and the optical facets prepared using ultra-precision ductile dicing, a process that we have previously demonstrated to

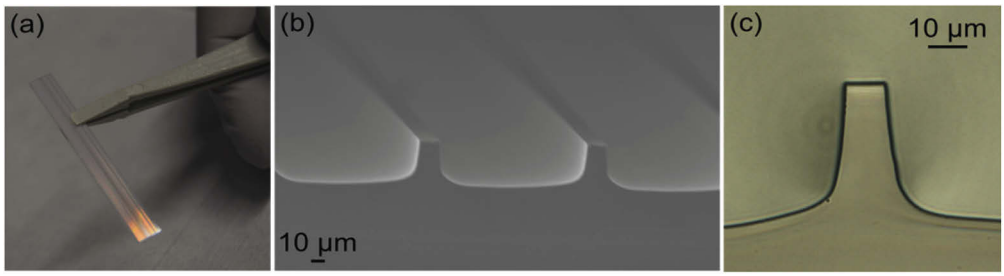

Fig. 1. (a) Image of 4.0 cm PPLN ridge waveguide with AR coating held in tweezers. (b) SEM of two waveguide facets [15]. (c) micrograph of waveguide facet [14].

Optics EXPRESS

achieve sub-nanometre surface roughness in lithium niobate [16]. Scanning electron microscope (SEM) and micrograph images of the resulting ridge waveguides are shown in Figs. 1(b) and 1(c) illustrating the optical quality of the dicing. Finally, the input and output facets of each chip are anti-reflection (AR) coated for both the 1560 nm pump and 780 nm SHG wavelengths. Further details of the fabrication process, including optimisation of indiffusion and dicing parameters for these wavelengths of operation are included in references [14–16].

4. Multi-watt experimental setup

Figure 2 details the experimental setup used to characterise our PPLN ridge waveguides at multi-watt power levels. Our pump source consists of a commercially available telecom tuneable laser source (TLS), which is injected into a polarizing maintaining (PM) 5 W erbium doped fibre amplifier (EDFA) via an in-line fibre polarizer. Light is launched into the ridge waveguide via a collimator and aspheric lens adjusted to achieve a similar spot size to the pump waveguide mode and thus maximise coupling efficiency. Pump polarization is adjusted to TM using a Glan-Thomson polarizing beam cube before waveguide launch. All launch optics are AR coated for the pump wavelength. At the output of the waveguides light is coupled and collimated via an aspheric lens. The pump and SHG beams are then split using a dichroic mirror; the residual pump is sent to a thermal power sensor and the SHG to a silicon power sensor through a neutral density (ND) filter. The ND filter loss was measured with the silicon power sensor and verified with the thermal power sensor measurements; the ND filter was measured to have a -83.3 ± 2.5% loss at 780 nm. The pump loss through our output coupling optics was measured as -17.6 ± 1.2% [15]. These losses are accounted for in the data presented in the following sections.

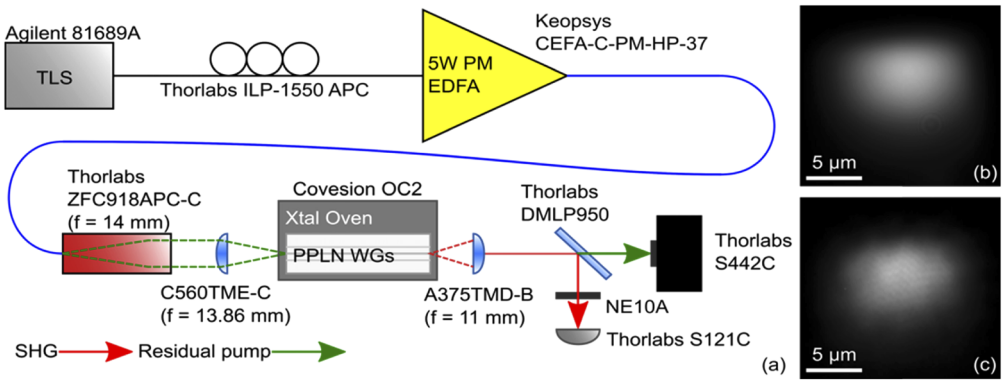

Fig. 2. (a) Optical characterisation setup used to collect SHG phase matching spectra by varying input wavelength for a range of incident pump powers. (b) and (c) are the mode profiles of the pump and SHG modes of a 12 µm wide ridge waveguide.

To characterise the SHG spectral profile and efficiency of our PPLN ridge waveguides the phase matching condition was varied by scanning the pump wavelength at various pump powers whilst measuring the SHG output power and residual pump from the device. The sample used in this work has a poling period of 18.5 µm and a 4.0 cm length (l) and was kept at a constant temperature throughout characterisation (114 °C) to minimise optical realignment due to thermal expansions in the optical setup. Each of the different waveguide widths on chip (11-13 µm) were first scanned at an incident pump of 300 mW to ascertain the waveguide with the highest SHG output power in the small conversion regime and to measure mode field diameters (MFDs) at the pump and SHG wavelengths. The 12 µm ridge width was found to phase match with the highest SHG output and had a MFD at the 1560 nm pump mode [Fig. 2(b)] of 10.0 µm and 8.8 µm for the x and y axes, respectively. The MFD for the 780 nm SHG mode [Fig. 2(c)] was

Optics EXPRESS

measured whilst phase matched by filtering the pump light, giving 9.9 µm and 8.3 µm for the x and y axes, respectively. The MFDs were collected using the same apparatus as discussed in [14]. The overlap integral [17] of the pump and SHG modes within the ridge waveguide is 98%, which is similar to that measured by Umeki *et al.* [5].

5. Waveguide characterisation

Characterisation of our PPLN waveguides at multi-watt CW operating powers in the large conversion regime was performed by incrementally increasing the pump power of our measurements up to 4.5 W. Figure 3 shows the resulting graph of SHG power versus pump power measured at the waveguide output, with the expected quadratic behaviour at low powers up to ~0.5 W of pump and changes to a linear dependence. A maximum SHG output of 2.50 ± 0.08 W was achieved for 3.37 ± 0.24 W of pump measured at the waveguide output (4.34 ± 0.30 W incident). The measurement uncertainties have been added to the power measurements and to the conversion efficiencies, ±7% and ±3% are the manufacturer's measurement uncertainties for the thermal and silicon optical power sensors, respectively. The crystal conversion efficiency steadily increases and plateaus at a maximum of 74 ± 5.6%, where $\eta_{\text{crystal}} = P_s/P_p(l)$x100 and $P_p(l)$ is measured far from phase matching. A device conversion efficiency of 58 ± 5.6%, was calculated, where $\eta_{device} = P_s/P_{in}$x100.

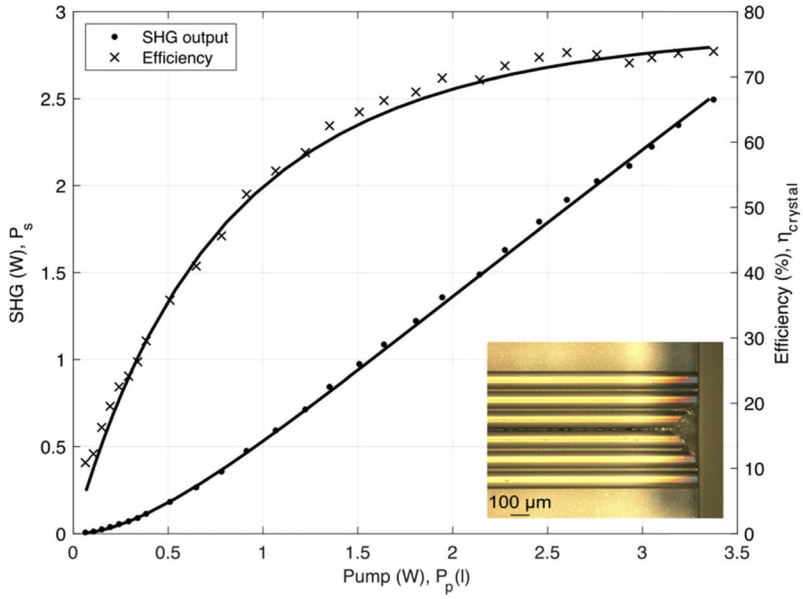

Fig. 3. Measured and modelled (solid lines) SHG output (spots) and efficiency (crosses) vs. pump power at the waveguide output. A maximum SHG output of 2.50 W was achieved for 3.37 W pump (4.34 W incident). This represents a 74% crystal conversion efficiency. Inset a micrograph of facet damage after being exposed to 4.50 W of incident pump power.

As the incident pump power in our devices is increased beyond 4.5 W the optical facet and ridge waveguide used in this experiment became damaged, as shown in the micrograph inset of Figure 3. Notice the conical damage at the input facet (right side of image), melting and reflowing of the ridge waveguide has also been seen at higher magnification. The failure mechanism at 4.5 W for this waveguide is under investigation.

Our result of 2.5 W of CW 780 nm SHG output power at 58% device efficiency in zinc-indiffused MgO:PPLN diced ridge waveguides represents improved power handling and operating

Optics EXPRESS

efficiency compared to similar devices fabricated using a bonding and thinned approach, which have been reported to operate up to 1.7W at 34% efficiency in a PPLN-on-LN format [7] or 1.0 W at 56% efficiency for PPLN-on-LT [5,6]. Analysis of our device behaviour in this large conversion regime is provided below.

6. SHG spectral narrowing

Using Eqs. (3) and (4) we follow the approach of Parameswaran *et al.* [4] by using numerical Runge-Kutta integration to model coupled mode equations incorporating propagation losses and an effective nonlinear coefficient. The solid lines in Figs. 3 and 4 are modelled based on numerical fitting to the experimental data. This approach allows us to relate our measured conversion efficiencies to operational waveguide parameters, given that there are uncertainties in the calculated effective refractive indices, modal overlaps, effective nonlinearity and propagation losses. In our model the crystal conversion efficiency was approximated by numerical solving of Eqs. (3) and (4) and then optimised using a Nelder–Mead simplex search method. A fit to Fig. 3 was achieved by varying the coupling efficiency (ξ) and optimising the parameters of effective nonlinearity (d_{eff}) and propagation losses at the SHG (α_s) and pump (α_p) wavelengths. To calculate the mode overlap integral (Iov) the MFDs in Fig. 2 were evaluated using Eq. (6). To estimate an initial condition for optimisation, ξ was subtracted from a measured insertion loss and the remaining loss divided by the waveguide length to give an initial value of α_p. The other initial values were: $\alpha_s = 2\alpha_p$ [4] and $d_{eff} = 14$ pm/V [18]. An insertion loss of -1.2 ± 0.06 dB was measured for this waveguide by comparing the incident and residual pump power off phase matching for each spectrum collected within the data set used to plot Fig. 3, here a mean is taken over the data set and the error is generated by taking the standard deviation. The coupling efficiency was calculated by evaluating the mode mismatch of the waveguide pump mode and that of a Gaussian spot from a lens launch, from which the overlap integral [17] was calculated to be 94%. This value of 94% is the upper limit of the achievable coupling efficiency. To allow for experimental misalignment within our model ξ was varied in percent steps from 94% to 80%, and a $\xi = 88\%$ yielded the lowest sum of residuals. After optimisation and fitting to the measured data in Fig. 3, we determine values of $\alpha_p = 0.12$ dB/cm, $\alpha_s = 0.58$ dB/cm, and a $d_{eff} = 7.6$ pm/V, the d_{eff} being a similar value measured by Wang *et al.* [19]. To show consistency between measured spectra and the ability for our model to predict spectral narrowing; we have plotted measured results from the small and large conversion regimes along with modelling in Fig. 4.

Using the results and model above, Figs. 4(a) and 4(b) plot our measured and theoretical SHG phase matching spectra for the small and large conversion regimes of operation, respectively. Figure 4(a) has the expected sinc^2 shape for phase matching in the small conversion regime and has a calculated nonlinear drive of $\Gamma = 21.3$ for an SHG output power of 0.113 ± 0.003 W. Figure 4(b) shows spectral narrowing of the sinc^2 profile, which is predicted via Eqs. (3) and (4) for the large conversion regime and results in an expected increase to $\Gamma = 53.6$ for an SHG output of 2.50 ± 0.08 W. Γ in Figure 4 has been calculated by evaluating $\Gamma = \sqrt{\eta_o P_p(0)}$ and $\eta_o = \kappa^2 Iov^2$, using the optimised values of κ and Iov generated by the model for the small and large conversion regimes. When the bandwidths are compared between Figs. 4(a) and 4(b) the full width half maximum (FWHM) is reduced by 35.7% in the large conversion regime. Figures 4(c) and 4(d) show the measured residual pump and its depletion with phase matching; notice the magnitude of depletion corresponds to the SHG output.

All spectra in Figure 4 have been normalized in the x axis for ease of comparison as our model described in section 2 does not account for thermal detuning caused by linear absorption. All detuning of our measured spectra is red shifted as input power is increased, which we attribute to linear absorption and heating of the waveguide. No blue detuning was measured, which would have indicated photorefractive damage as reported by Pal *et al.* in Ti indiffused PPLN waveguides [8]. PPLN waveguides doubling to 671 nm at 2.4 W with an internal efficiency of 54% have

Optics EXPRESS

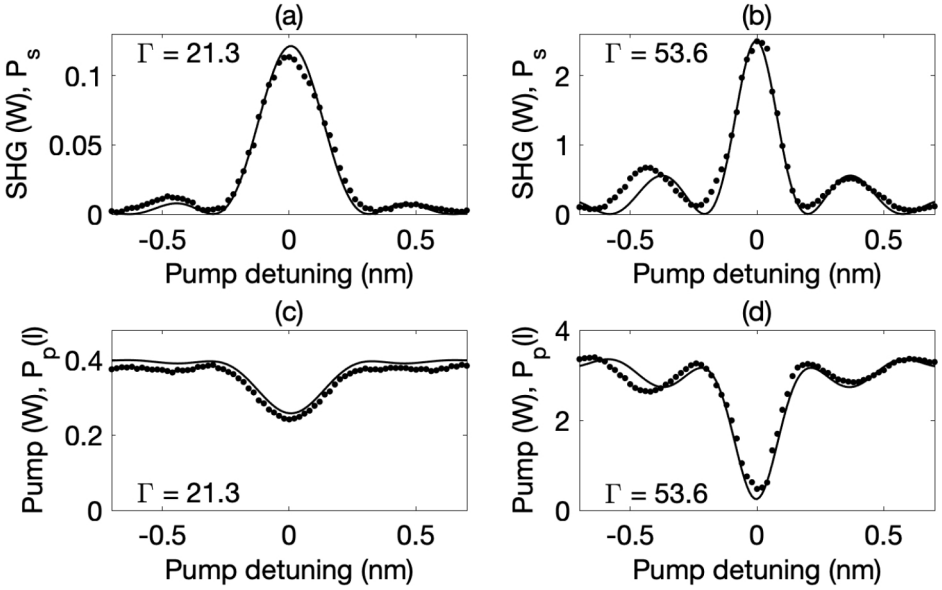

Fig. 4. Measured (spots) and modelled (solid lines) phase matching spectra and pump depletion from a PPLN ridge waveguide operating in the small (a)(c) and large (b)(d) conversion regimes. Figures 4(a) and (c) was recorded at a SHG output of 0.113 ± 0.003 W resulting in a calculated nonlinear drive of $\Gamma = 21.3$, with a FWHM of 0.28 nm. Figures 4(b) and (d) were recorded at our maximum SHG output of 2.50 ± 0.08 W corresponding to a nonlinear drive of $\Gamma = 53.6$ and a FWHM of 0.18 nm. The x-axis wavelength tuning range of all plots has been normalized and compensated for thermal effects to enable comparison as the model does not account for phase matching wavelength change from absorption.

been demonstrated and did show a phase matching spectrum that departed from the sinc^2 at 2.4 W [20]. However, asymmetry shown in their phase matching spectrum was accounted for by light absorption mechanisms causing inhomogeneous heating within the waveguide at the SHG wavelength of 671 nm, rather than the nonlinear drive explanation we give here. Equations (3) and (4) also do not account for SHG spectral changes caused by imperfections in waveguide fabrication, which can cause asymmetry in the side lobes and a departure from the expected symmetrical SHG intensity profile [5,21,22].

The spectra in Figs. 4(a) and 4(b) show clear similarities to those calculated by Eckardt *et al.* in [3] where conversion efficiency of a modelled bulk PPLN crystal at 56% is shown to have a sinc^2 spectrum and at 99% the central peak is narrowed with increased amplitude of side lobes. In work by Parameswaran *et al.*, spectral narrowing of a PPLN waveguide was previously demonstrated and fitted with good theoretical agreement [4,11], albeit to a laser that was only 'on' for 1/20,000 of CW (50 ns at 1 kHz) and with an average power at least four orders of magnitude lower. Here, our results demonstrate the first reported measurement of spectral narrowing in a PPLN waveguide operating in the large conversion regime with a true CW source.

7. Conclusion

We have demonstrated CW spectral narrowing in a zinc indiffused MgO:PPLN diced ridge waveguide performing 1560 nm SHG with an output power of 2.5 W at 780 nm and crystal conversion efficiency of 74% (device efficiency 58%), the highest reported power and efficiency combination in a waveguide of this type to date. We have modelled conversion efficiency,

Optics EXPRESS

showing excellent agreement to experimental data and fit to SHG spectra in both the small and large conversion regimes. Spectral narrowing of up to 35.7% was measured as nonlinear drive is increased in the large conversion regime. This device represents a new platform for PPLN waveguides that can generate SHG output powers at the multi-watt level with >50% conversion efficiencies.

Funding

Innovate UK (102805, 104000, 104613); Engineering and Physical Sciences Research Council (EP/M013294/1, EP/M024539/1, EP/P034160/1, EP/R041636/1).

Acknowledgments

The authors would like to acknowledge the support of Neil Sessions for assistance with cleanroom processing. Corin Gawith acknowledges support from the Royal Academy of Engineering Senior Research Fellowship scheme.

Disclosures

SAB + LGC: Covesion Ltd. (C,P), PGRS + CBEG: Covesion Ltd. (E,P). The authors declare no conflicts of interest.

References

1. J. A. Armstrong, N. Bloembergen, J. Ducuing, and P. S. Pershan, "Interactions between Light Waves in a Nonlinear Dielectric," Phys. Rev. **127**(6), 1918–1939 (1962).
2. D. Eimerl, "High average power harmonic generation," IEEE J. Quantum Electron. **23**(5), 575–592 (1987).
3. R. Eckardt and J. Reintjes, "Phase matching limitations of high efficiency second harmonic generation," IEEE J. Quantum Electron. **20**(10), 1178–1187 (1984).
4. K. R. Parameswaran, J. R. Kurz, R. V. Roussev, and M. M. Fejer, "Observation of 99% pump depletion in single-pass second-harmonic generation in a periodically poled lithium niobate waveguide," Opt. Lett. **27**(1), 43–45 (2002).
5. T. Umeki, O. Tadanaga, and M. Asobe, "Highly efficient wavelength converter using direct-bonded PPZnLN ridge waveguide," IEEE J. Quantum Electron. **46**(8), 1206–1213 (2010).
6. T. Lévèque, L. Antoni-Micollier, B. Faure, and J. Berthon, "A laser setup for rubidium cooling dedicated to space applications," Appl. Phys. B **116**(4), 997–1004 (2014).
7. C.-W. Hsu, R. Lai, C.-S. Hsu, Y.-T. Huang, K. Wu, and M.-H. Chou, "Efficient, watt-level frequency doubling and optical parametric amplification on periodically poled lithium niobate ridge waveguide," Proc. SPIE **10902**, 109020D (2019).
8. S. Pal, B. K. Das, and W. Sohler, "Photorefractive damage resistance in Ti:PPLN waveguides with ridge geometry," Appl. Phys. B **120**(4), 737–749 (2015).
9. W. M. Young, R. S. Feigelson, M. M. Fejer, M. J. F. Digonnet, A. F. Marshall, and H. J. Shaw, "Photorefractive-damage-resistant Zn-diffused waveguides in MgO:LiNbO3," Opt. Lett. **16**(13), 995–997 (1991).
10. W. M. Young, M. M. Fejer, M. J. F. Digonnet, A. F. Marshall, and R. S. Feigelson, "Fabrication, characterization and index profile modeling of high-damage resistance Zn-diffused waveguides in congruent and MgO:lithium niobate," J. Lightwave Technol. **10**(9), 1238–1246 (1992).
11. K. R. Parameswaran, "Thesis: Highly Efficient Optical Frequency Mixers," Stanford University (2002).
12. R. L. Byer, "Parametric Oscillators and Nonlinear Materials," in *Nonlinear optics: proceedings of the Sixteenth Scottish Universities Summer School in Physics 1975*, P. G. Harper and B. S. Wherrett eds., (Academic Press, 1977).
13. R. Regener and W. Sohler, "Efficient second-harmonic generation in Ti:LiNbO3 channel waveguide resonators," J. Opt. Soc. Am. B **5**(2), 267–277 (1988).
14. L. G. Carpenter, S. A. Berry, R. H. S. Bannerman, A. C. Gray, and C. B. E. Gawith, "ZnO indiffused MgO:PPLN ridge waveguides," Opt. Express **27**(17), 24538–24544 (2019).
15. S. A. Berry, L. G. Carpenter, A. C. Gray, P. G. R. Smith, and C. B. E. Gawith, "Zn-indiffused diced ridge waveguides in MgO:PPLN generating 1 watt 780 nm SHG at 70% efficiency," OSA Continuum **2**(12), 3456–3464 (2019).
16. L.G. Carpenter, S.A. Berry, and C. B. E. Gawith, "Ductile dicing of LiNbO3 ridge waveguide facets to achieve 0.29 nm surface roughness in single process step," Electron. Lett., **53**(25), 1672–1674 (2017).
17. R. Hunsperger, *Integrated Optics Theory and Technology* (Springer-Verlag, New York, 2009), Chap 7.
18. Covesion Ltd., "Covesion Guide to PPLN Material," https://www.covesion.com/support/covesion-guide-to-ppln/material-properties-of-lithium-niobate.html.

Optics EXPRESS

19. L. Wang, C. E. Haunhorst, M. F. Volk, F. Chen, and D. Kip, "Quasi-phase-matched frequency conversion in ridge waveguides fabricated by ion implantation and diamond dicing of MgO:LiNbO3 crystals," Opt. Express **23**(23), 30188–30194 (2015).
20. N. Kretzschmar, U. Eismann, F. Sievers, F. Chevy, and C. Salomon, "2.4-watts second-harmonic generation in ppZnO:LN ridge waveguide for lithium laser cooling," Opt. Express **25**(13), 14840–14855 (2017).
21. A. C. Gray, S. A. Berry, L. G. Carpenter, J. C. Gates, P. G. R. Smith, and C. B. E. Gawith, "Investigation of PPLN Waveguide Uniformity via Second Harmonic Generation Spectra," IEEE Photonics Technol. Lett. **32**(1), 63–66 (2020).
22. M. Santandrea, M. Stefszky, V. Ansari, and C. Silberhorn, "Fabrication limits of waveguides in nonlinear crystals and their impact on quantum optics applications," New J. Phys. **21**(3), 033038 (2019).